Estimating Patient Dose from X-ray Tube Output Metrics:

Automated Measurement of Patient Size from CT Images Enables Large-scale Size-specific Dose Estimates[1]

Ichiro Ikuta, MD, MMSc
Graham I. Warden, MD
Katherine P. Andriole, PhD
Ramin Khorasani, MD, MPH
Aaron Sodickson, MD, PhD

Purpose: To test the hypothesis that patient size can be accurately calculated from axial computed tomographic (CT) images, including correction for the effects of anatomy truncation that occur in routine clinical CT image reconstruction.

Materials and Methods: Institutional review board approval was obtained for this HIPAA-compliant study, with waiver of informed consent. Water-equivalent diameter (D_W) was computed from the attenuation-area product of each image within 50 adult CT scans of the thorax and of the abdomen and pelvis and was also measured for maximal field of view (FOV) reconstructions. Linear regression models were created to compare D_W with the effective diameter (D_{eff}) used to select size-specific volume CT dose index ($CTDI_{vol}$) conversion factors as defined in report 204 of the American Association of Physicists in Medicine. Linear regression models relating reductions in measured D_W to a metric of anatomy truncation were used to compensate for the effects of clinical image truncation.

Results: In the thorax, D_W versus D_{eff} had an R^2 of 0.51 (n = 200, 50 patients at four anatomic locations); in the abdomen and pelvis, R^2 was 0.90 (n = 150, 50 patients at three anatomic locations). By correcting for image truncation, the proportion of clinically reconstructed images with an extracted D_W within ±5% of the maximal FOV D_W increased from 54% to 90% in the thorax (3602 images) and from 95% to 100% in the abdomen and pelvis (6181 images).

Conclusion: The D_W extracted from axial CT images is a reliable measure of patient size, and varying degrees of clinical image truncation can be readily corrected. Automated measurement of patient size combined with CT radiation exposure metrics may enable patient-specific dose estimation on a large scale.

[1] From the Department of Radiology and Center for Evidence Based Imaging, Brigham and Women's Hospital, 75 Francis St, Boston, MA 02115 (I.I., G.I.W., K.P.A., R.K., A.S.); Harvard Medical School, Boston, Mass (I.I., G.I.W., K.P.A., R.K., A.S.); Department of Radiology, Norwalk Hospital, Norwalk, Conn (I.I.); and United States Air Force, Washington, DC (G.I.W.). From the 2012 RSNA Annual Meeting. Received December 10, 2012; revision requested January 25, 2013; final revision received June 27; final version accepted July 22. **Address correspondence to** A.S. (e-mail: *asodickson@partners.org*).

The content is solely the responsibility of the authors and does not necessarily represent the official views of the National Library of Medicine or the National Institutes of Health.

Concerns about the potential risks of radiation exposure from computed tomography (CT) have captured the attention of the medical community and of the public as a whole (1–4). The California legislature responded by mandating the recording of "patient dose" in the radiology report, which became effective on July 1, 2012 (5). Informatics toolkits have been developed to collect radiation exposure data from individual examinations (6–8) and to provide the automation necessary to aggregate individual information for large-scale study (9). Recording CT scanner metrics, such as the volume CT dose index ($CTDI_{vol}$) and the dose-length product, can aid in successfully monitoring x-ray tube output, but these metrics fall short of measuring radiation dose to the patient (10–12). For a given CT technique, patient dose decreases as patient size increases because there is more attenuation of the incident x-ray beam by surrounding soft tissues, necessitating adjustment according to patient size for appropriate CT dosimetry (13–17).

There are many patient safety and quality improvement applications of large-scale radiation exposure databases (6,18). Certain activities, including regulatory oversight, institutional benchmarking, and some CT quality assurance and protocol optimization efforts, can be performed by using large databases devoid of patient size information. However, several efforts either further benefit from or require the inclusion of patient size information. Protocol optimization efforts and appropriate dose-alert levels should ideally be linked to patient size to identify undesirable variations in technique arising from poorly standardized CT protocols (19) while controlling for the expected large variations necessary to maintain image quality at all patient sizes (20). While patient-specific dose monitoring and risk assessment remain controversial in large part because of uncertainties in our underlying cancer risk models (21,22), any such programs would require more accurate patient dosimetry than can be derived from the raw CT exposure metrics $CTDI_{vol}$ and dose-length product. Furthermore, efforts to directly test or refine our risk models of the biological effects of ionizing radiation at the low doses used in diagnostic imaging will benefit from large databases of accurate dosimetry data linked to cancer or other biological outcomes (23–26).

The American Association of Physicists in Medicine (AAPM) report 204 established a method to calculate size-specific dose estimates (SSDEs) by size-adjusting $CTDI_{vol}$ (14). Multiplication of the $CTDI_{vol}$ by the appropriate conversion factor (derived from Monte Carlo simulations and phantom measurements) yields the SSDE, which is intended to better approximate radiation dose to the patient's central organs. To implement this type of approach on a large scale, automated methods to determine patient size are needed.

The purpose of this study was to test the hypothesis that patient size can be accurately calculated from axial CT images, including correction for the effects of anatomy truncation that occur in routine clinical CT image reconstruction.

Advances in Knowledge

- Patient size may be modeled as a water-equivalent diameter (D_W), which can be automatically extracted from axial CT images and used to calculate size-specific dose estimates.
- The extracted D_W values correlate well with the physical dimensions of effective diameter (R^2 of 0.90 for abdomen and pelvis, $P < 1 \times 10^{-15}$; R^2 of 0.51 for thorax, $P < 1 \times 10^{-15}$) while taking into account variations in tissue attenuation and morphologic features between anatomic regions.
- The reconstructed field of view in routine clinical practice often truncates peripheral anatomy and leads to underestimation of D_W; correction for this effect may be achieved by capturing a measure of image truncation, resulting in an increase in D_W values to within ±5% of the true D_W from 54% to 90% for thoracic CT images and from 95% to 100% for abdominal and pelvic CT images.

Implications for Patient Care

- Patient size metrics are essential to properly translate CT metrics of x-ray tube output into size-specific dose estimates that are more meaningful for an individual patient.
- The automated capture of size information such as D_W from CT images may enable large-scale patient-specific dosimetry estimation for patients of variable geometry and tissue attenuation.

Materials and Methods

Institutional review board approval was obtained for this Health Insurance Portability and Accountability Act–compliant study, with waiver of informed consent.

Setting and Cohort

The cohort included patients of 18 years of age or older of both sexes who underwent CT in January 2012 in the

Published online before print
10.1148/radiol.13122727 **Content codes:** CT PH IN

Radiology 2014; 270:472–480

Abbreviations:
AAPM = American Association of Physicists in Medicine
$CTDI_{vol}$ = volume CT dose index
D_{eff} = effective diameter
DICOM = Digital Imaging and Communications in Medicine
D_W = water-equivalent diameter
FOV = field of view
SSDE = size-specific dose estimate

Author contributions:
Guarantors of integrity of entire study, I.I., A.S.; study concepts/study design or data acquisition or data analysis/interpretation, all authors; manuscript drafting or manuscript revision for important intellectual content, all authors; approval of final version of submitted manuscript, all authors; literature research, I.I., G.I.W., A.S.; clinical studies, I.I.; experimental studies, I.I., G.I.W., K.P.A.; statistical analysis, I.I., K.P.A.; and manuscript editing, all authors

Funding:
This research was supported by the National Institutes of Health (grants R01LM010679 and T15LM007092).

Conflicts of interest are listed at the end of this article.

Brigham and Women's Hospital (Boston, Mass) Emergency Department (approximately 60 000 visits per year). The first 50 CT examinations of the thorax and the first 50 CT examinations of the abdomen and pelvis that met inclusion criteria were analyzed.

Image Reconstruction

The emergency radiology CT scanner (Somatom Definition AS+; Siemens Healthcare, Forchheim, Germany) was calibrated daily with a water phantom for clinical use. CT scans were reconstructed at 3-mm axial section thickness by radiologic technologists, using a routine clinical reconstruction field of view (FOV) (clinical FOV). Additional axial series with 3-mm section thickness were reconstructed at the CT scanner workstation with the maximal 500-mm FOV (maximal FOV), and all images were transferred to the archive (Centricity; GE Healthcare, Piscataway, NJ) serving the picture archiving and communication system. Scans were excluded if the entire contour of the skin was not visible on the maximal FOV reconstruction (39 of the thorax, 23 of the abdomen and pelvis) because of miscentering, broad shoulders, or obese habitus or if the scan was obtained with the arms at least partially down in the scanned region rather than overhead (20 of the thorax, two of the abdomen and pelvis).

Patient Size Definitions, Study Metrics, and Measurement Methods

The *effective diameter* (D_{eff}), as defined in AAPM report 204 (14), is the diameter of a circle containing the same cross-sectional area as that of an ellipse with axes defined by the anteroposterior and lateral dimensions of the patient (Eq [1]). The maximal midline skin-to-skin dimensions along the patient's anteroposterior and lateral dimensions were manually measured at the picture archiving and communication system from the axial images reconstructed with the maximal FOV, without attempting to correct for irregularities in the skin surface owing to undulating skin contours, as may occur with breast tissue (Fig 1). One author (I.I.) performed these measurements during his 2nd year as an informatics fellow. D_{eff} is the geometric mean of these diameters taken from axial images:

$$D_{eff} = \sqrt{D_{AP} \cdot D_L}, \quad (1)$$

where D_{AP} is anteroposterior diameter and D_L is lateral diameter.

The *water-equivalent diameter* (D_W) represents the diameter of a cylinder of water that contains the same total x-ray attenuation as that contained within the patient's axial cross section and depends on both the cross-sectional area of the patient and the attenuation of the contained tissues (Fig 2) (17,27–29); D_W may be calculated from the CT images as Equation (2):

$$D_W = \sqrt{\sum_{n\,\text{pixels}}^{i=1} \left(\frac{HU_i + 1000}{1000}\right) \cdot (X \cdot Y) \cdot \left(\frac{4}{\pi}\right)}, \quad (2)$$

where HU signifies Hounsfield units, X is pixel width, and Y is pixel height.

Each pixel's attenuation value in Hounsfield units is normalized to a new scale with an attenuation of one for water and zero for air. All pixels with attenuation less than −600 HU are presumed to represent pure air, to correct for variations in manufacturer conventions, some of which set air outside the patient to −1024 rather than −1000 HU. These normalized attenuation values are multiplied by the pixel area (pixel width multiplied by pixel height) and summed over all pixels in the image. Multiplication of this normalized attenuation-area product by $4/\pi$ followed by a square root operation yields the D_W.

The *air border proportion* is the proportion of image border pixels that contain an attenuation value less than −600 HU. If the entire patient cross section is fully contained within the reconstructed FOV, the air border proportion would be one (Fig 3). As the peripheral soft tissues are truncated in reduced FOV reconstructions, the air border proportion decreases.

The *proportion of maximal FOV* D_W is the ratio of the D_W measured on routine clinical images to the D_W measured on images reconstructed at maximal FOV, shown schematically in Figure 3. As greater amounts of the patient are truncated by the clinical FOV, there is a corresponding decrease in the measured D_W, as part of the patient's anatomy is excluded from measurement in the CT image.

Figure 1

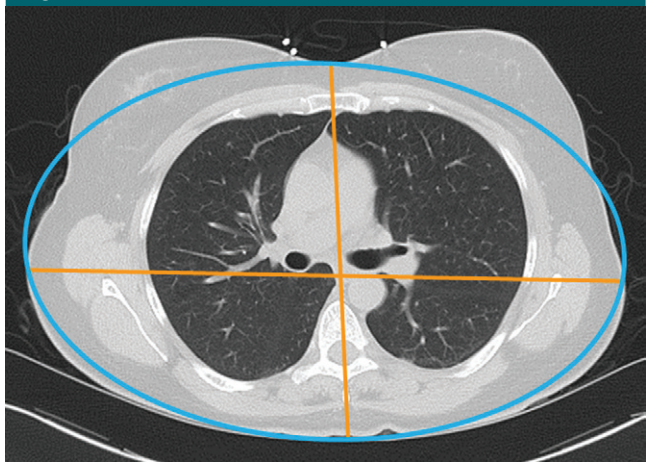

Figure 1: D_{eff} measurements in a female patient. The anteroposterior and lateral dimensions (orange) are measured skin to skin and may be used to create an ellipse (blue) with the same minor and major axes. However, this patient's anatomic contours are not geometrically regular, and her breast tissue lies outside of the ellipse.

Figure 2

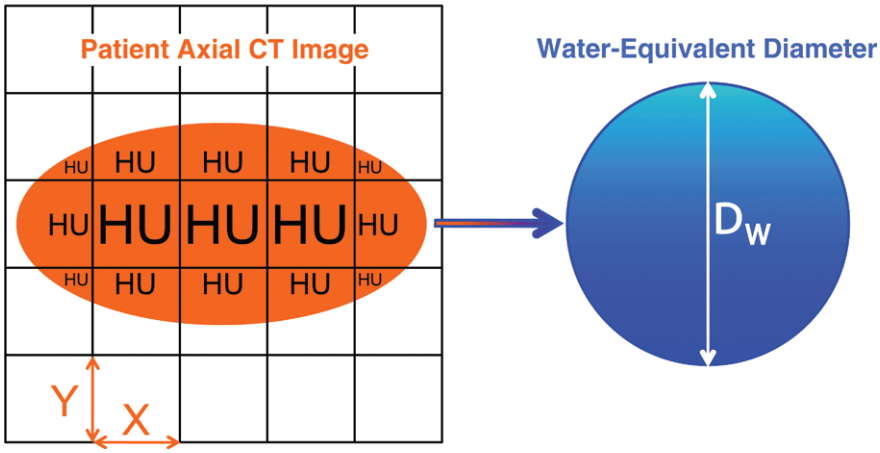

Figure 2: D_W calculation. The patient axial CT image (left, orange) is comprised of individual pixels with width (*X*), height (*Y*), and CT numbers (measured in Hounsfield units *[HU]*). As in Equation (2), pixel attenuations are normalized so that a pixel has an attenuation defined as zero if it contains air and one if it contains water. Subsequent multiplication by the pixel area ($X \cdot Y$) yields the normalized attenuation-area product, which is converted from a rectangular to a circular attenuation-area product when multiplying by $4/\pi$. A square root operation then yields the diameter of a cylinder of water, D_W (right, blue), that would contain the same total attenuation as the CT image.

These methods of calculating D_W and the air border proportion were coded into a previously reported open-source informatics toolkit–the generalized radiation observation kit, or GROK (6,30), configured to analyze the desired CT images. The toolkit calculates D_W by obtaining pixel attenuation values in Hounsfield units from the axial CT images and pixel dimensions from the Digital Imaging and Communications in Medicine (DICOM) header (Eq [2]). The air border proportion is calculated for each CT image by "thresholding" the 1-pixel-wide image border (the pixel is designated as air or not air on the basis of its value above or below -600 HU).

Patient Size Surrogates: D_W versus D_{eff}

For each of the 50 CT scans of the thorax, D_W and D_{eff} were measured on images at four anatomic locations: the lung apex, the superior aspect of the aortic arch, the carina, and immediately superior to the diaphragm. For each of the 50 CT scans of the abdomen and pelvis, D_W and D_{eff} were measured on images at three anatomic locations: the superior mesenteric artery, immediately superior to the iliac crest, and at the L5-S1 intervertebral disk space.

The AAPM report 204 (14) defined $CTDI_{vol}$ conversion factors, or CF, with Equation (3), as follows:

$$CF = a \cdot e^{-b \cdot D_{eff}}, \qquad (3)$$

where *a* and *b* are coefficients. For the standard 32-cm-diameter CT dose index phantom used for reporting of torso exposures, they derived coefficients $a = 3.704$ and $b = 0.0367$, and used Equation (3) to produce a lookup table of conversion factors at representative D_{eff} values (14). The measured D_{eff} can be used to select the appropriate conversion factor, which is then multiplied by the reported $CTDI_{vol}$ to produce the SSDE.

Linear regression models were created to define the relationship between D_W and D_{eff} separately for the thorax and for the abdomen and pelvis.

Image Truncation Prevalence and Correction

The toolkit was used to measure D_W for all images in the clinically reconstructed CT series (which sometimes truncated peripheral anatomy) and at the corresponding locations in the maximal FOV reconstructions (which always included the entire patient contour). For a training set including all images from the first 10 CT scans, linear regression models were created separately for the thorax and for the abdomen and pelvis to define the relationship between the proportion of maximal FOV D_W and the air border proportion. These regression model fit equations predict how much of the patient's total tissue attenuation remains in the image on the basis of the measured air border proportion, allowing for correction of the *measured* D_W (from truncated images) to the *expected* D_W in the absence of truncation. This correction was applied to a validation set including all images from the remaining 40 clinically reconstructed CT scans to determine the percentage of the corrected D_W values within ±5% of the corresponding maximal FOV D_W values.

Statistical Analysis

Statistical analysis and graphics were generated by using spreadsheet software (Excel 2007; Microsoft, Seattle, Wash) and the statistical software R (version 2.15.0; R Foundation for Statistical Computing, Vienna, Austria). Linear regression was performed with $\alpha = .05$.

Results

Surrogates of Patient Size: D_W versus D_{eff}

Figure 4 shows the correlation and linear regressions relating the automatically extracted D_W to the manually measured D_{eff}. For the thorax, 200 images from 50 scans at four anatomic locations had a D_{eff} range of 21.3–33.6 cm ($R^2 = 0.51$, $P < 1 \times 10^{-15}$). For the abdomen and pelvis, 150 images from 50 scans at three anatomic locations had a D_{eff} range of 24.8–36.5 cm ($R^2 = 0.90$, $P < 1 \times 10^{-15}$). The linear models for both the thorax and the abdomen and pelvis were significant, with correlation between D_W and D_{eff} that was good in the thorax and excellent in the

Figure 3

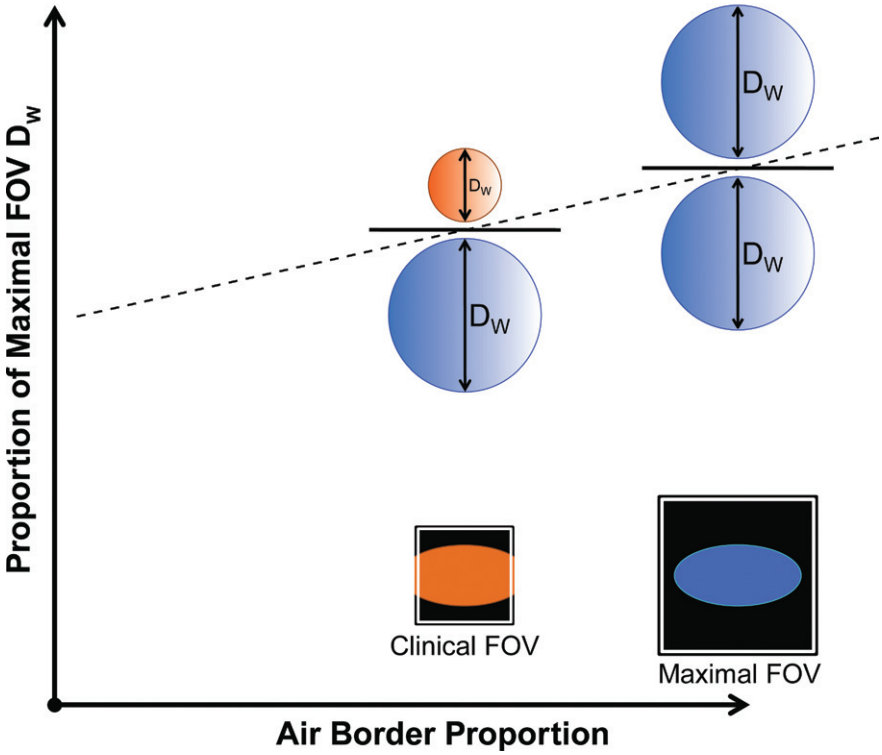

Figure 3: Effect of clinical image truncation. The air border proportion is the proportion of image border pixels that contain attenuation values less than −600 HU. If there is no image truncation (schematic patient contour as blue ellipse with maximal FOV), the air border proportion is one (all border pixels contain air), resulting in extraction of the full patient D_W (blue circles). In routine clinical image reconstruction, the peripheral soft tissues are often truncated (orange ellipse with clinical FOV) to focus on the anatomy of interest, resulting in a reduced air border proportion, and a reduced D_W (orange circle).

Figure 4

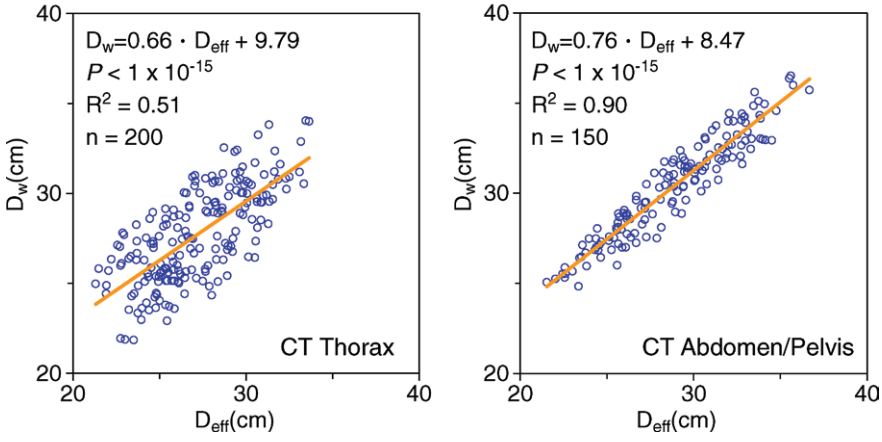

Figure 4: Patient size correlation. D_W demonstrates excellent correlation with D_{eff} for the abdomen and pelvis and good correlation for the thorax.

abdomen and pelvis. As demonstrated in Figure 5, *A*, and 5, *B*, the aerated lungs yielded a smaller D_W than an abdominal or pelvic image with comparable D_{eff}, which contains more soft-tissue attenuation and less internal air.

Image Truncation Prevalence and Correction

As patient tissue traverses the image border and decreases the air border proportion, there is a progressive decrease in measured D_W below the maximal FOV D_W (Fig 6). There is substantial variation, depending on the body habitus of the patient and the quantity and attenuation of the truncated anatomy: The notable divergence in the thorax as the air border proportion decreases relates in part to the observation that the same amount of truncated soft tissue has a larger proportional effect in the mid thorax where there is less total contained attenuation than in the shoulders or upper abdomen where there is little contained gas. Nonetheless, the significant linear regression models show good correlation both in the thorax (R^2 = 0.72, $P < 1 \times 10^{-15}$) and in the abdomen and pelvis (R^2 = 0.74, $P < 1 \times 10^{-15}$).

Use of the linear fit equations of Figure 6 to correct the measured D_W to the expected maximal FOV D_W on the basis of the air border proportion yields the results in the Table. Before correction, 54% (1942 of 3602) and 95% (5893 of 6181) of the truncated images in the thorax and in the abdomen and pelvis, respectively, had a D_W within ±5% of the maximal FOV D_W. After applying the correction procedure based on the linear model for each anatomic region, 90% (3250 of 3602) of thoracic images and 100% (6154 of 6181) of the abdominal and pelvic images had a corrected D_W within ±5% of the maximal FOV D_W.

Discussion

We found that accurate measurement of patient size from axial CT images can be automated, including calculation of D_W and correction for the effects of image truncation encountered in clinical routine. When combined

Figure 5

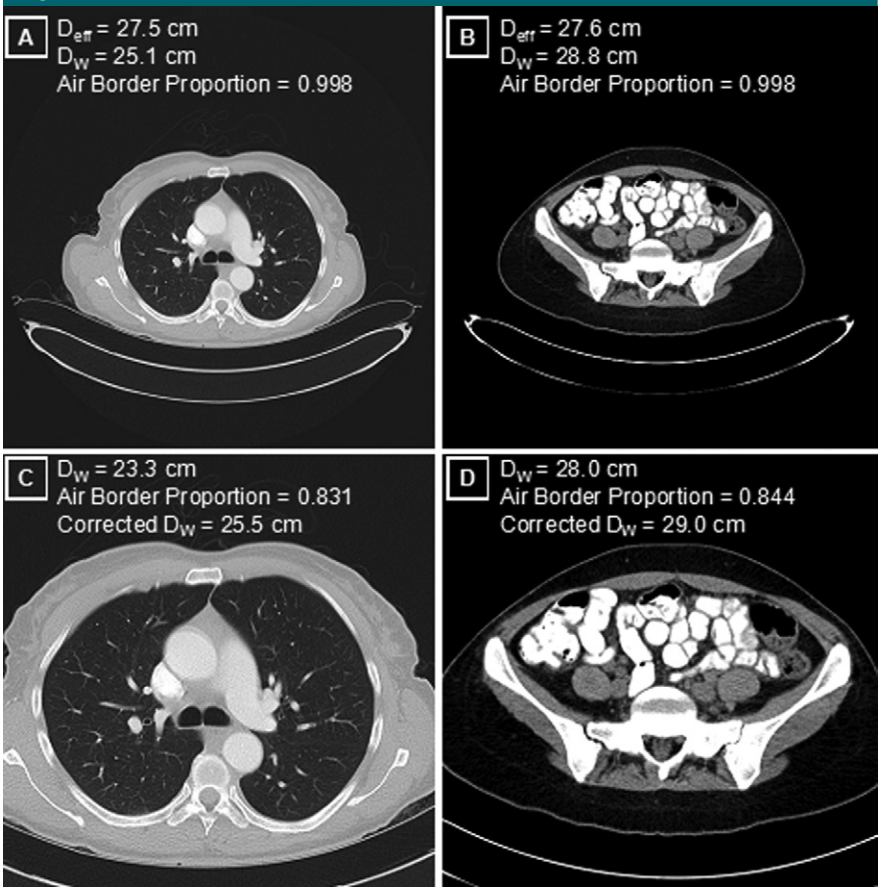

Figure 5: Patient size and image truncation. *A,* Maximal FOV axial reconstructions in the thorax and, *B,* those in the pelvis for patients with comparable manually measured D_{eff}. While the physical areas of these two axial cross sections are similar, the D_W is 15% higher in the pelvis (*B*) than in the thorax (*A*) because of the aerated lungs, corresponding to a 32% higher tissue attenuation in the pelvis (contained attenuation scales as the square of the diameter). Physical dimensions such as D_{eff} do not capture this underlying attenuation difference. *C, D,* Axial image reconstructions performed in clinical routine with a limited FOV have expected decreases in the measured D_W, compared with reconstructions in *A* and *B*. Image *C* is truncated version of *A*; image *D* is truncated version of *B*. Use of the air border proportion as a measure of truncation allows for the correction of D_W values that more closely approximate maximal FOV images.

with automated extraction of CT scanner x-ray tube output metrics, patient- and size-specific radiation dose monitoring initiatives may be enabled in large scale.

Many metrics of patient size, including weight (15,31), body mass index (32), cross-sectional diameter (33), and perimeter (13), have been used previously for CT dosimetry calculations. The D_{eff}, as selected by the AAPM, is a reasonable choice for manual measure, but it has limitations in regions of irregular body contours that deviate from an elliptical shape, cannot be directly measured in regions of image truncation, and does not account for variations in the x-ray attenuation of heterogeneous tissues within the body. Two cross sections through the body with identical outer diameters would have the same measured D_{eff} and, thus, the same AAPM report 204 size correction factors, even though in reality a more air-filled body region would typically have greater central organ doses, as there is less tissue to attenuate the incident x-rays (34).

We, instead, selected D_W for automated patient size measurement because it captures variations in contained tissue attenuation and more closely matches the automated tube-current–modulation calculations performed on most CT scanners from the localizer images. The intent of automated D_W extraction is to provide a robust measure of patient attenuation that can be used for SSDE calculation in place of the purely geometric measure, D_{eff}. It should be noted that, in AAPM report 204, only abdominal organ doses were evaluated as a function of the D_{eff} of the abdomen and the extension of these methods to the thoracic organs was not formally validated. Within the abdomen, D_W and D_{eff} correlate quite closely, and the derivation methods underlying AAPM report 204 suggest that use of D_W in place of D_{eff} is a reasonable approach. While we expect that this proposed replacement and extension of SSDE methods to the thorax would also improve generalizability to the thorax, both of them require formal validation from a dosimetry perspective.

Because D_W intentionally measures a different quantity than D_{eff}, the linear relationship between these metrics is not perfect. For a given patient, one would expect D_W to be relatively insensitive to the degree of inspiration (as the total contained tissue attenuation is unchanged), although D_{eff} will increase as the chest wall expands. Variable ratios of aerated lung to soft tissue also produce greater variability between patients in the average tissue attenuation within the chest compared with that in the abdomen and pelvis. These factors contribute to the looser correlation between D_W and D_{eff} in the thorax (R^2 = 0.51) compared with that in the abdomen and pelvis (R^2 = 0.90).

The increasing proportion of low-attenuation fat in large patients flattens the slope of the Figure 4 linear fit models below one and contributes to their nonzero intercepts. The aerated lungs in the thorax produce a smaller D_W than in the abdomen for a given D_{eff}, further reducing the slope of the linear fit equation in the thorax. In keeping with this observation, recent

Figure 6

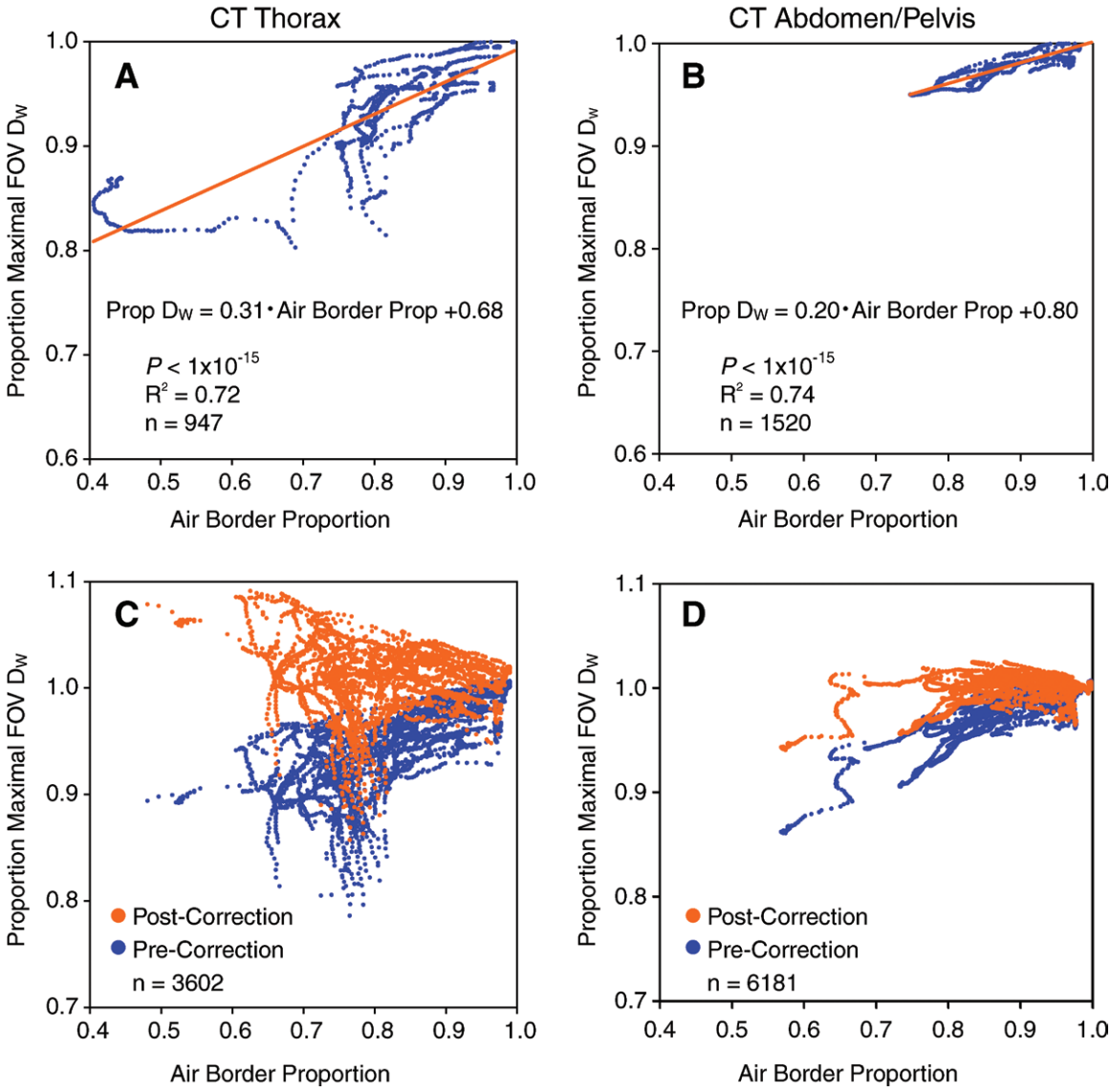

Figure 6: Linear regression model correction for image truncation. For each image in the thorax and in the abdomen and pelvis, the corresponding point plots the ratio of the measured D_W to the maximal FOV D_W along the y-axis and the air border proportion on the x-axis. As in Figure 3, the air border proportion is a measure of image truncation, and greater degrees of image truncation (moving to the left on the x-axis) result in extracted D_W values progressively smaller than the maximal FOV D_W. *A,* Thorax and, *B,* abdomen and pelvis training set data (10 patients each) used to define the linear regression models relating the measured D_W and degree of truncation to the expected maximal FOV D_W. Validation data sets in 40 patients each in the thorax *(C)* and abdomen and pelvis *(D),* where the linear regression models are used to correct the clinical FOV truncated D_W values (data in blue) to the predicted maximal FOV D_W values (data in orange).

work by Wang et al (29) demonstrated that geometry-based size-estimation methods that do not account for aerated lung may lead to a substantially overestimated D_W, compared with attenuation-based methods such as the method implemented in this work.

It should be noted that, in our implementation, the measured D_W captures all of the attenuation contained in the image. This includes variable amounts of the CT table that artificially increase the measured attenuation, typically contributing 4–5 cm of D_W, which systematically adds to the Figure 4 model intercepts and increases the overall patient attenuation (proportional to the square of D_W) by a few percentage points. Future methodologic enhancements to more accurately determine D_W could include body contour

Clinical Image Truncation Rates and Correction

Anatomy Imaged	Truncated Clinical FOV Images	Corrected Image D_W Values
Thorax	54 (1942/3602)	90 (3250/3602)
Abdomen and pelvis	95 (5893/6181)	100 (6154/6181)

Note.—Data are percentages of images within ±5% of maximal FOV D_w, and numbers in parentheses are numbers of images used to calculate the percentages. Percentages were rounded.

segmentation to remove CT table attenuation, although it should be noted that the CT table is included in the projection radiograph attenuation measurements used by the CT manufacturers to plan automated tube-current modulation during the scan.

The issue of clinical FOV image truncation must be dealt with to automate any size extraction methods, as it is common to exclude peripheral soft tissues from the reconstructed images. Prospectively adding maximal FOV image reconstructions is not practical or appropriate to clinical practice and is not retrospectively available on archived scans. Truncation correction methods are most important to increase accuracy of D_W measurements in the thorax, where the more peripheral distribution of attenuating tissues results in proportionately larger truncation effects than in the more uniformly distributed abdominal tissues. While our linear regression correction of Figure 6 does tend to overshoot for high degrees of anatomy truncation in the thorax, it nonetheless improves D_W estimation substantially. To put this in context, on the basis of the AAPM report 204 correction factors for the adult patient sizes represented in this study, a 5% measurement error in the D_W or D_{eff} value would be expected to produce a corresponding error in the associated SSDE correction factors on the order of 5%.

Physical dimensions needed for D_{eff} can be extracted from planning projection radiograph images, which are not typically truncated, but frontal and lateral planning images are not always obtained. However, measuring patient attenuation and, thus, D_W requires direct knowledge or reverse engineering of the proprietary image processing steps used by each manufacturer (27,29). Most manufacturers do, in fact, calculate patient attenuation from these projection radiographs as the basis for tube-current–modulation algorithms. Ideally, these calculated D_W values should be obtained at the scanner and included in the DICOM attributes for each image, with the average values over the scan range stored as part of radiation dose DICOM structured reports and in the DICOM attributes of the screen-capture CT dose reports. Doing so would obviate the need to calculate these size metrics, after the fact, from reconstructed axial images and would inherently eliminate any need to account for patient truncation (except in situations where the patient anatomy extends beyond the maximal reconstruction FOV).

Our study had some limitations. We did not explicitly validate the automated D_W measurements with different CT scanner models, but we would not expect this factor to have a substantial effect because pixel Hounsfield unit scales are standardized, and quality control tolerance checks are performed daily. As our validation scans were all performed in adults, our truncation correction and size translation methods cannot necessarily be extrapolated to pediatric patient sizes or to patient populations with fundamentally different body habitus. In addition, our validation excluded scans with any degree of truncation on the maximal FOV reconstructions. While in most such cases, this was caused by small amounts of lateral truncation in the shoulders or hips, some of the excluded scans were obtained in our most obese patients.

In summary, patient size determination is an essential element to convert CT scanner x-ray tube output metrics into meaningful measures of patient dose. We developed a method to automatically extract patient size from axial CT images as a water-equivalent diameter D_W, including correction for the image truncation of peripheral soft tissues that is common in clinical routine. Such automated patient size extraction may enhance large-scale radiation databases with SSDEs, thus enabling new opportunities in radiation dose monitoring and potentially aiding efforts to refine our radiation risk models.

Disclosures of Conflicts of Interest: I.I. No relevant conflicts of interest to disclose. **G.I.W.** No relevant conflicts of interest to disclose. **K.P.A.** Financial activities related to the present article: none to disclose. Financial activities not related to the present article: received reimbursement for travel to committee meetings from RSNA Radiology Informatics Committee, RSNA QIBA, ACR Information Technologies and Informatics Committee, and SIIM Program Committee; serves as Associate Editor for the Journal of Digital Imaging without receiving payment. Other relationships: none to disclose. **R.K.** No relevant conflicts of interest to disclose. **A.S.** No relevant conflicts of interest to disclose.

References

1. Brenner DJ, Hall EJ. Computed tomography: an increasing source of radiation exposure. N Engl J Med 2007;357(22):2277–2284.
2. Sodickson A, Baeyens PF, Andriole KP, et al. Recurrent CT, cumulative radiation exposure, and associated radiation-induced cancer risks from CT of adults. Radiology 2009;251(1):175–184.
3. Berrington de González A, Mahesh M, Kim KP, et al. Projected cancer risks from computed tomographic scans performed in the United States in 2007. Arch Intern Med 2009;169(22):2071–2077.
4. Fazel R, Krumholz HM, Wang Y, et al. Exposure to low-dose ionizing radiation from medical imaging procedures. N Engl J Med 2009;361(9):849–857.
5. Padilla A, Alquist EK. California Senate Bill 1237. http://info.sen.ca.gov/pub/09-10/bill/sen/sb_1201-1250/sb_1237_bill_20100929_chaptered.html. Published February 19, 2010. Accessed September 1, 2011.
6. Sodickson A, Warden GI, Farkas CE, et al. Exposing exposure: automated anatomy-specific CT radiation exposure extraction for quality assurance and radiation monitoring. Radiology 2012;264(2):397–405.

7. Cook TS, Zimmerman SL, Steingall SR, Maidment ADA, Kim W, Boonn WW. RADIANCE: An automated, enterprise-wide solution for archiving and reporting CT radiation dose estimates. RadioGraphics 2011;31(7):1833–1846.

8. Shih G, Lu ZF, Zabih R, et al. Automated framework for digital radiation dose index reporting from CT dose reports. AJR Am J Roentgenol 2011;197(5):1170–1174.

9. Prevedello LM, Sodickson AD, Andriole KP, Khorasani R. IT tools will be critical in helping reduce radiation exposure from medical imaging. J Am Coll Radiol 2009;6(2):125–126.

10. McCollough CH, Leng S, Yu L, Cody DD, Boone JM, McNitt-Gray MF. CT dose index and patient dose: they are not the same thing. Radiology 2011;259(2):311–316.

11. McCollough CH. Automated data mining of exposure information for dose management and patient safety initiatives in medical imaging. Radiology 2012;264(2):322–324.

12. Bankier AA, Kressel HY. Through the Looking Glass revisited: the need for more meaning and less drama in the reporting of dose and dose reduction in CT. Radiology 2012;265(1):4–8.

13. Turner AC, Zhang D, Khatonabadi M, et al. The feasibility of patient size-corrected, scanner-independent organ dose estimates for abdominal CT exams. Med Phys 2011;38(2):820–829.

14. American Association of Physicists in Medicine. Size-specific dose estimates (SSDE) in pediatric and adult body CT examinations. Report 204. AAPM Task Group 204 of the Diagnostic Imaging Council CT Committee. College Park, Md: American Association of Physicists in Medicine, 2011.

15. Israel GM, Cicchiello L, Brink J, Huda W. Patient size and radiation exposure in thoracic, pelvic, and abdominal CT examinations performed with automatic exposure control. AJR Am J Roentgenol 2010;195(6):1342–1346.

16. Huda W, Vance A. Patient radiation doses from adult and pediatric CT. AJR Am J Roentgenol 2007;188(2):540–546.

17. Menke J. Comparison of different body size parameters for individual dose adaptation in body CT of adults. Radiology 2005;236(2):565–571.

18. Committee on Tracking Radiation Doses from Medical Diagnostic Procedures; Nuclear and Radiation Studies Board. Division on Earth and Life Studies; National Research Council. Tracking Radiation Exposure from Medical Diagnostic Procedures: workshop reports. Washington, DC: National Academies Press, 2012.

19. Smith-Bindman R, Miglioretti DL, Johnson E, et al. Use of diagnostic imaging studies and associated radiation exposure for patients enrolled in large integrated health care systems, 1996-2010. JAMA 2012;307(22):2400–2409.

20. Hricak H, Brenner DJ, Adelstein SJ, et al. Managing radiation use in medical imaging: a multifaceted challenge. Radiology 2011;258(3):889–905.

21. Committee to Assess Health Risks from Exposure to Low Levels of Ionizing Radiation, National Research Council. Health risks from exposure to low levels of ionizing radiation: BEIR VII phase 2. Washington, DC: National Academies Press, 2006.

22. Hendee WR, O'Connor MK. Radiation risks of medical imaging: separating fact from fantasy. Radiology 2012;264(2):312–321.

23. Pearce MS, Salotti JA, Little MP, et al. Radiation exposure from CT scans in childhood and subsequent risk of leukaemia and brain tumours: a retrospective cohort study. Lancet 2012;380(9840):499–505.

24. Boone JM, Hendee WR, McNitt-Gray MF, Seltzer SE. Radiation exposure from CT scans: how to close our knowledge gaps, monitor and safeguard exposure—proceedings and recommendations of the Radiation Dose Summit, sponsored by NIBIB, February 24-25, 2011. Radiology 2012;265(2):544–554.

25. Mathews JD, Forsythe AV, Brady Z, et al. Cancer risk in 680,000 people exposed to computed tomography scans in childhood or adolescence: data linkage study of 11 million Australians. BMJ 2013;346:f2360.

26. Sodickson A. CT radiation risks coming into clearer focus [editorial]. BMJ 2013;346:f3102.

27. Li B, Behrman RH, Norbash AM. Comparison of topogram-based body size indices for CT dose consideration and scan protocol optimization. Med Phys 2012;39(6):3456–3465.

28. Wang J, Duan X, Christner JA, Leng S, Yu L, McCollough CH. Attenuation-based estimation of patient size for the purpose of size specific dose estimation in CT. I. Development and validation of methods using the CT image. Med Phys 2012;39(11):6764–6771.

29. Wang J, Christner JA, Duan X, Leng S, Yu L, McCollough CH. Attenuation-based estimation of patient size for the purpose of size specific dose estimation in CT. II. Implementation on abdomen and thorax phantoms using cross sectional CT images and scanned projection radiograph images. Med Phys 2012;39(11):6772–6778.

30. How GROK Works & Source Code Download - CEBI - BWH Radiology Department. http://www.brighamandwomens.org/Research/labs/cebi/GROK/default.aspx. Accessed January 13, 2012.

31. Miyoshi T, Kanematsu M, Kondo H, et al. Abdomen: angiography with 16-detector CT—comparison of image quality and radiation dose between studies with 0.625-mm and those with 1.25-mm collimation. Radiology 2008;249(1):142–150.

32. Dey D, Nakazato R, Pimentel R, et al. Low radiation coronary calcium scoring by dual-source CT with tube current optimization based on patient body size. J Cardiovasc Comput Tomogr 2012;6(2):113–120.

33. Ogden K, Huda W, Scalzetti EM, Roskopf ML. Patient size and x-ray transmission in body CT. Health Phys 2004;86(4):397–405.

34. Cheng PM. Automated estimation of abdominal effective diameter for body size normalization of CT dose. J Digit Imaging 2013;26(3):406–411.